PROCEEDINGS OF SCIENCE

Study the measurement of air depth of shower maximum for cosmic rays by LHAASO-WFCTA

Lingling Ma[a,*] **and Liping Wang**[a,b]

[a] *Key Laboratory of Particle Astrophysics & Experimental Physics Division & Computing Center, Institute of High Energy Physics, Chinese Academy of Sciences*
100049, Beijing, China

E-mail: llma@ihep.ac.cn, wanglp@ihep.ac.cn

According to the superposition model, the air depth at which the shower size reaches its maximum (X_{max}) is sensitive to the mass compositions of cosmic rays, so X_{max} can be used to identify the mass compositions and measure the average mean logarithm mass of cosmic rays. The Wide Field of view Cherenkov Telescope Array (WFCTA) as an important part of Large High Altitude Air Shower Observatory can record the Cherenkov images which can be used to reconstruct X_{max}. The angular distance ($Dist$) between the arriving direction and the gravity center of the Cherenkov image is related to X_{max}. In this work, the method of the X_{max} reconstruction is studied by simulation data, and $20g/cm^2$ resolution of X_{max} can be achieved. The ability of the reconstructed X_{max} in mass composition identification and the measurement of the mean logarithm mass is also studied.

38th International Cosmic Ray Conference (ICRC2023)
26 July - 3 August, 2023
Nagoya, Japan

*Speaker

PoS(ICRC2023)407

1. Introduction

Since the discovery of cosmic rays has been more than one century, the mechanisms of their origin, acceleration and propagation has still been remain unclear. It is commonly assumed that the galactic cosmic rays are produced by the shock acceleration in supernova remnants since they can provide the energy budget for cosmic ray acceleration. The accurate measurements of mass compositions of cosmic rays and their energy spectra around the "knee" region can help to resolve the century puzzles.

For cosmic rays with energies below 100 TeV, they can be observed by space-based experiments, like AMS02, and high-altitude balloons, like CREAM. However, as the increase of the energy of cosmic rays, their flux drops rapidly, at higher energies, the flux is too low for direct observation, and the observation of these cosmic rays can only be realized by the ground-burn experiments via the observation of extensive air showers (EAS), such as KASCDE, ARGO-YBJ, Auger. However, during the development of EAS, the primary information of cosmic rays, such as, the primary energy and the mass have been lost, completely. Among the reconstructions of these primary information, the mass reconstruction is the most difficult one for the EAS experiments. In one hand, the mass can only be inferred from the EAS features which carry the mass information, but suffer large intrinsic fluctuations. So the small average differences between neighboring mass compositions are often overwhelmed. In other hand, the deductions of mass from the EAS features should depend on the comparison between the experiment and the air shower simulation. The air shower simulation suffers the uncertainties of high energy interaction models and the uncertainties of the composition models of cosmic rays.

The features of EAS which are sensitive to the primary mass composition can be deduced from the superposition model. In the model, the nucleus with atomic number A and total energy E_0 is taken to be A individual single nucleons, each with energy E_0/A [1]. According to the superposition model, the number of muons N_μ in the air shower and the air depth X_{max} at which the the number of electrons and photons in the air shower reaches its maximum are sensitive to the mass compositions.

The X_{max} can be measured by the observation of Fluorescence or Cherenkov light in the EAS. By using the fluorescence telescopes, like Auger and TA [2], the longitudinal development of the air shower can be measured, and the X_{max} can be measured directly. The slope of the lateral distribution of the Cherenkov light also has been used to measure the X_{max} by using the non-imaging Cherenkov detectors such as CASA-BLANCA [3] and Tunka [4].

The Large High Altitude Air Shower Observatory is located at Haizi Muontain, Daocheng, Sichuan, China at an altitude of approximately 4410 m above sea leval, corresponds an air depth of 600 g/cm^2[5]. The LHAASO consists of three main detector arrays: the 1.3 square-kilometer array (KM2A)of electromagnetic particle and muon detectors[6], water Cherenkov detector array (WCDA)[7] with a total area of 78,000 m^2, and Wide filed-of-view (FoV) Cherenkov telescope array (WFCTA) [8] consisting of 18 telescopes. With the combined observation of the different type detectors, LHAASO can measure multiple parameters of the EAS simultaneously. This study investigated the method for X_{max} reconstruction by using the observation of WFCTA. The descriptions of the detectors of WFCTA and KM2A and the simulations are presented in section 2. The method for the X_{max} reconstruction is presented in section 3. The applications of the

reconstructed X_{max} is described in section 4. Finally, the conclusions are presented in section 5.

2. Detectors and Simulation

The telescopes of WFCTA are designed to collect and image the atmospheric Cherenkov light emitted by the charged particles in the EAS. The camera of each telescope is made up of 32×32 SiPMs with a square light funnel in front of it. The FoV of each pixel is about $0.5^\circ \times 0.5^\circ$, so the total FoV of the telescope is about $16^\circ \times 16^\circ$. To cover a wider FoV, the telescops of the WFCTA are arranged closly on the ground, and they span different directions in the azimuth direction. In order to cover the energy range from 100 TeV to 100 PeV, the observation stage of the WFCTA is divided into two stages. The fist stage is the combined observation of the first six telescopes with the first half KM2A and the first water pool of WCDA; the second stage is the combined observation of all of the 18 telescope and the whole KM2A and WCDA array. The Cherenkov images recorded by the telescope is used to reconstruct the X_{max}.

CORSIKA with version 7.4000 is used to generate the EAS events. The Cherenkov option is used, so both the Cherenkov and secondary particle information is recorded to simulate the combined observation of WFCTA and KM2A. The Hadronic interaction models QGSJET-II-04 and FLUKA are used to simulate the hadronic interactions for energies below and above 100 GeV.

Five mass compositions proton helium CNO MgAlSi and ironwith energy ranges from 100 TeV to 1 PeV and from 1 PeV to 10 PeV are generated. In order to increase the statistics of high energy events, the spectral index of the power-law function (-1) is used. The fluxes of the five composition groups are weighted by the Gaisser (H3a) composition model.

3. X_{max} reconstruction

3.1 $Dist$ sensitive to X_{max}

The Cherenkov light suffers less scattering during its propagation to the telescope, the arriving direction of the Cherenkov light contains the information of the production altitude of it considering the geometry between the telescope, the shower's core location and the arriving direction of the shower axis. The altitude corresponding to the arriving direction with the largest number of Cherenkov photons is near the X_{max}.

The top 20 brightest SiPMs are used to calculate the gravity center of the image (x_c, y_c) on the focal plane of the telescope. The arriving directions of the EAS reconstructed by KM2A is in the horizontal coordinates. To obtain the angular distance ($Dist$) between the gravity center and the arriving direction, the Euler rotation is used to transform the arriving direction to the focal plane of the telescope, denoted as (x_s, y_s). The $Dist$ can be calculated by function 1.

$$Dist = \sqrt{(x_c - x_s)^2 + (y_c - y_s)^2} \tag{1}$$

$Dist$ is related to the distance from X_{max} to the telescope. The smaller of the zenith angle, the smaller distance is expected, as shown in Fig. 1. In order to eliminate the affects of the zenith angle, the parameter $Dist/cos(\theta)$, denoted as $Dist_0$, is used, here θ indicates the zenith angle.

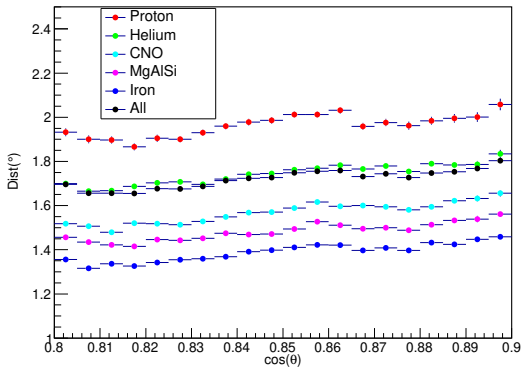

Figure 1: The dependence of *dist* on the zenith angle. The meanings of the different color dots are described in the plot.

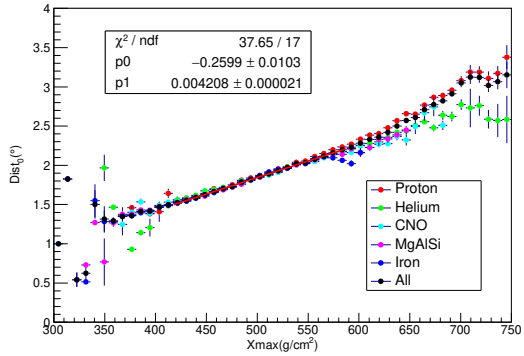

Figure 2: The relationship between the $Dist_0$ and X_{max} for different mass compositions. The meanings of the different colors are also shown in the plot. The relationship of all mass compositions with ratio 1:1:1:1:1 is fitted by a linear function.

Due to the geometry effect, the parameter $Dist_0$ is larger for events with larger R_p. For a given R_p range, for example 100 m $< R_p <$ 105 m, $Dist_0$ and X_{max} has a linear relationship as shown in Fig.2. According to Fig.2, the relationship is hardly dependent on the mass compositions, so the ratio of the five mass compositions with 1:1:1:1:1 is used to fit the relationship by a linear function ($p1 \times X_{max} + p0 = Dist_0$), which is used to reconstruct the X_{max}. The linear relationship is fitted for each R_p range with width 5 m.The fitting results of $p0$ and $p1$ in each R_p bin are shown in Fig. 3(a) and Fig. 3(b).

3.2 X_{max} Resolution

Based on the linear relationship between $Dist_0$ and X_{max}, the X_{max} can be reconstructed. The distributions of the divations of the reconstructed X_{max}^{rec} and the real X_{max}^{real} ($X_{max}^{rec} - X_{max}^{real}$) for the five mass compositions in the energy range from 10^6-$10^{6.1}$ GeV are shown in Fig.4(a). The RMS of the distributions can be considered as the resolution of X_{max} reconstruction. The resolutions of the X_{max} reconstruction for the five mass compositions are shown in Fig.4(b) which are the function of

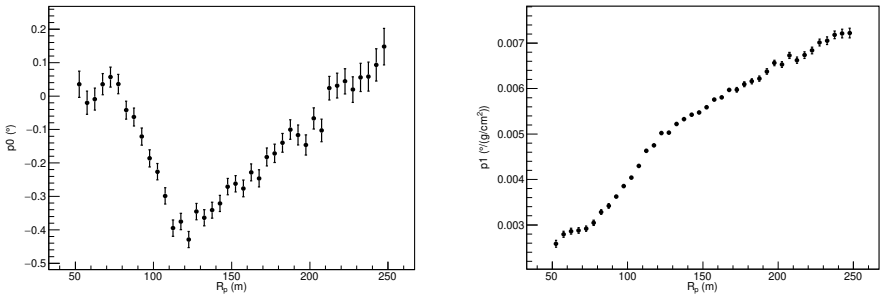

(a) (b)

Figure 3: The fitting results in each R_p bin of the relationship between $Dist_0$ and R_p.(a) the fitting results of $p0$; (b) the fitting results of $p1$.

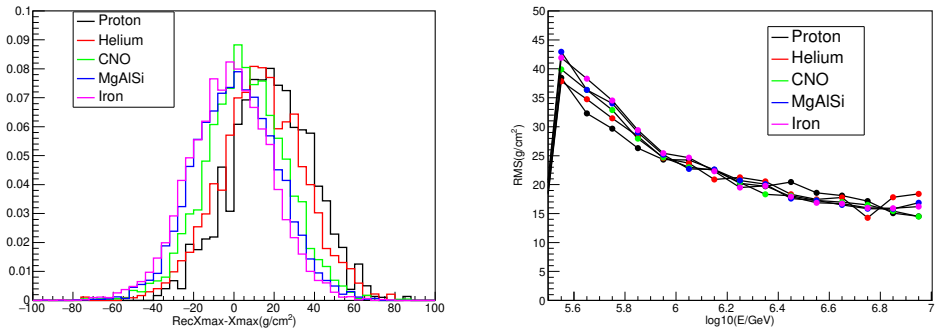

(a) (b)

Figure 4: (a) The distributions of the deviations of the reconstructed X_{max}^{rec} and the real X_{max}^{real} ($X_{max}^{rec} - X_{max}^{real}$) for different mass compositions in the energy range from $10^{6.0}$-$10^{6.1}$ GeV; (b) The resolutions of X_{max} reconstruction for five mass compositions versus the energy. Different color lines and shapes are described in the plot.

the primary energy. According to Fig.4(b), the resolution of the X_{max} reconstruction is improved as the energy increasing, and is independent on the energy. The resolution of the X_{max} resolution is about $25 g/cm^2$ around 1 PeV, is about $20 g/cm^2$ around 10 PeV.

4. Application of X_{max}

According to the superposition model, the X_{max} initiated by cosmic ray nucleus with mass A can be described by $X_{max}^{A} = X_{max}^{p} - \lambda_r \ln A$, approximately, here,$X_{max}^{p}$ is the X_{max} initiated by the proton, λ_r is the radiation length. So the X_{max} is sensitive to the primary mass composition of cosmic rays, and can be used to discriminate the mass compositions of cosmic rays and to measure the mean logarithm mass <lnA> of cosmic rays .

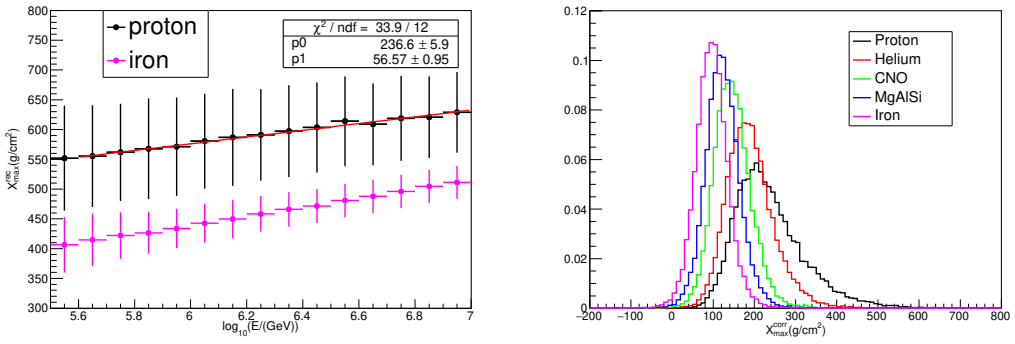

(a) (b)

Figure 5: (a) The relationship between the reconstructed X_{max} and primary energy for protons and irons. (b) The distributions of the X_{max}^{rec} with the corrections of the elongation for five compositions in the energy range from $10^{5.5}$ GeV to 10^{7} GeV. The meanings of the different colors are described in the plot.

4.1 Discrimination of mass composition

Although the X_{max} of cosmic rays is sensitive to its mass compositions, it also relies on its primary energy, since X_{max}^{p} increases as the increase of the logarithm primary energy $\log_{10}(E)$, which is called elongation rate. The increases of the reconstructed X_{max} as the primary energy for protons and irons are presented in Fig. 5(a), which can be fitted by a linear function as shown by the red line in the plot. The slop of the linear function indicates the elongation rate, , which is about 56. In order to show the X_{max}^{rec}'s ability of the mass discrimination, the RMS of the distributions of the X_{max}^{rec} in each energy bin is shown in the plot. The RMS includes two contributions, one is the intrinsic fluctuation of X_{max}, the other one is the resolution of the X_{max} reconstruction. In this work, the elongation rate of protons is used to eliminate X_{max}'s dependence on energy. The distributions of the X_{max}^{rec} with the corrections of the elongation for five compositions in the energy range from $10^{5.5}$ GeV to 10^{7} GeV are shown in Fig. 5(b).

The ability of X_{max}^{rec} to discriminate proton, proton plus helium (light mass composition) or iron are studied in detail as shown in Fig. 6(a) 6(b) 6(c). A parameter $\sigma = \frac{|mean_1 - mean_2|}{\sqrt{rms_1^2 + rms_2^2}}$ is defined to measure the discriminate ability of X_{max}^{corr}. The σ is about 0.8, 1.0, 1.2, respectively, for proton - others, light - others and iron - others with energy around 1 PeV.

4.2 $< lnA >$ measurement

Since the X_{max} for cosmic rays is related to its number of mass (A), X_{max} can be used to calculate the mean logarithm mass $< lnA >$. The changes of $< lnA >$ with its primary energy are related to the origin and propagation of cosmic rays. The relationship between the X_{max} and lnA for the five mass composition cosmic rays in the energy range from 10^{6} GeV to $10^{6.1}$ GeV is shown in Fig. 7(a). The relationship can be fitted by a linear function which is used to calculate <lnA>. According to the linear function, the <lnA> can be obtained for a individual composition as shown by the color squares in the plot. In addition, the <lnA> for all compositions based on Gaisser model

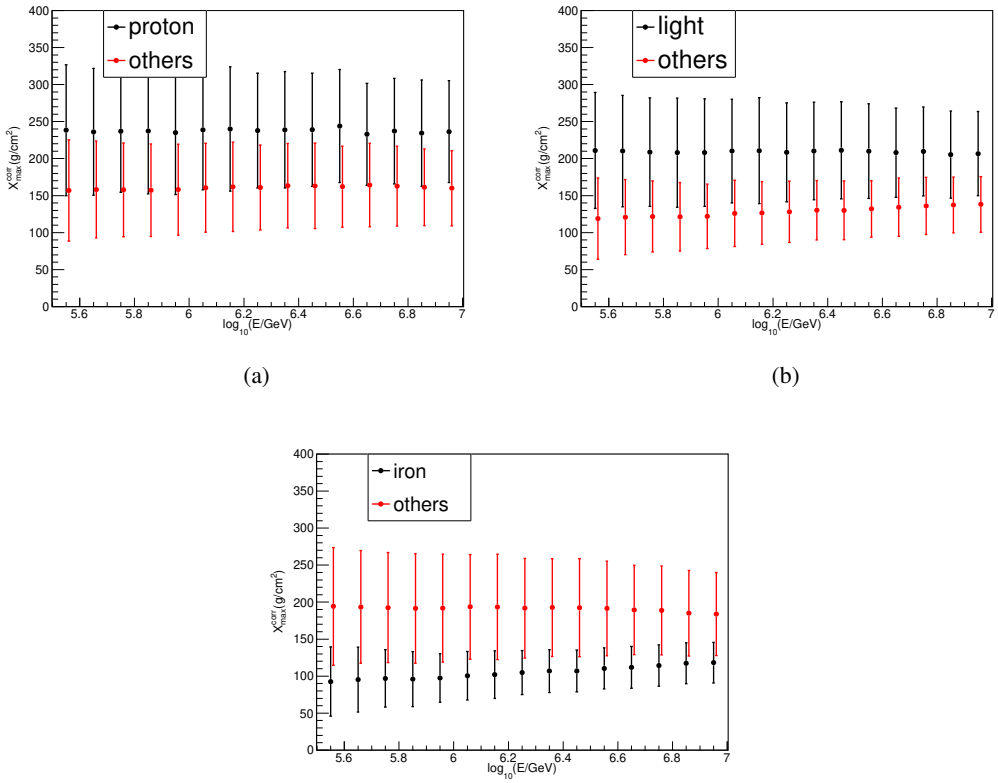

(a) (b)

(c)

Figure 6: (a) The relationship between the reconstructed X_{max} and primary energy for protons and irons. (b) The distributions of the X_{max}^{rec} with the corrections of the elongation for five compositions in the energy range from $10^{5.5}$ GeV to 10^7 GeV. The meanings of the different colors are described in the plot.

can also be obtained as shown by the black dots in the plot. According to the plot, the calculated <lnA> is consistent with the expectation based on the Gaisser model.

5. summary and discussion

The method of the reconstruction of X_{max} is study based on the observation of WFCTA. The The resolution is about $25g/cm^2$ around 1 PeV, and is about $20g/cm^2$ around 10 PeV for all the mass compositions.

The X_{max} is a mass sensitive parameter according to the superposition model. In this work, the ability of X_{max} to discriminate the protons, light component, irons are studied. In addtion, the X_{max} can also be used to measure the <lnA>.

References

[1] Matthews, J. . (2005). A heitler model of extensive air showers. Astroparticle Physics, 22(5-6), 387-397.

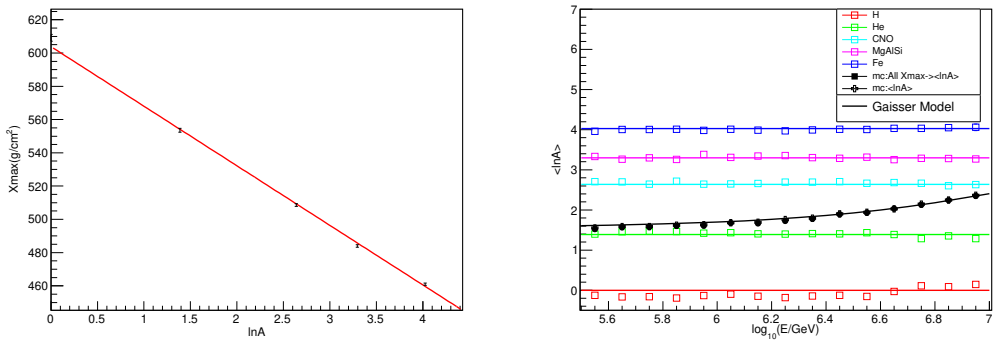

(a) (b)

Figure 7: (a) The relationship between the reconstructed X_{max} and $< lnA >$ for the five mass compositions in the energy range from 10^6 GeV to $10^{6.1}$ GeV. The redline is the fitting results of the relationship based on a linear function . (b) The <lnA> calculated based on the linear function shown in 7(a). The color squares are the results based on an individual assumption while the black dots are the results based on Gaisser model. The meanings of the different colors are described in the plot.

[2] Yushkov, A. , Bellido, J. , Belz, J. , De Souza, V. , Hanlon, W. , Ikeda, D. , et al. (2019). Depth of maximum of air-shower profiles: testing the compatibility of measurements performed at the pierre auger observatory and the telescope array experiment.

[3] Cassidy, M. , Fortson, L. F. , Fowler, J. W. , Ong, R. A. , Sommers, P. . (1997). CASA-BLANCA: A Large Non-imaging Cherenkov Detector at CASA-MIA. 10.48550/arXiv.astro-ph/9707038.

[4] Epimakhov, S. , Berezhnev, S. F. , Budnev, N. M. , Chiavassa, A. , Zagorodnikov, A. V. . (2013). Elemental composition of cosmic rays above the knee from xmax measurements of the tunka array.

[5] He, H. . (2009). LHAASO project: Detector design and prototype.

[6] Aharonian, F. , Cao, Z. , Stenkin, Y. V. , Collaboration, L. . (2021). Observation of the crab nebula with lhaaso-km2a a performance+study. Chinese Physics C, 45(2), 025002.

[7] Aharonian, F. , Cao, Z. , Stenkin, Y. V. , Collaboration, L. . (2021). Performance of lhaaso-wcda and observation of crab nebula as a standard candle. Chinese Physics C, 45(8), 16.

[8] Aharonian, F. , An, Q. , Axikegu, Bai, L. X. , Bai, Y. X. , Bao, Y. W. , et al. (2021). Absolute calibration of LHAASO WFCTA camera based on LED.